

Velocity continuation and the anatomy of residual prestack time migration^a

^aPublished in *Geophysics*, 68, 1650-1661 (2003)

*Sergey Fomel*¹

ABSTRACT

Velocity continuation is an imaginary continuous process of seismic image transformation in the post-migration domain. It generalizes the concepts of residual and cascaded migrations. Understanding the laws of velocity continuation is crucially important for a successful application of time migration velocity analysis. These laws predict the changes in the geometry and intensity of reflection events on migrated images with the change of the migration velocity. In this paper, I derive kinematic and dynamic laws for the case of prestack residual migration from simple geometric principles. The main theoretical result is a decomposition of prestack velocity continuation into three different components corresponding to residual normal moveout, residual dip moveout, and residual zero-offset migration. I analyze the contribution and properties of each of the three components separately. This theory forms the basis for constructing efficient finite-difference and spectral algorithms for time migration velocity analysis.

INTRODUCTION

The conventional approach to seismic migration theory (Claerbout, 1985; Berkhout, 1985) employs the downward continuation concept. According to this concept, migration extrapolates upgoing reflected waves, recorded on the surface, to the place of their reflection to form an image of subsurface structures. Post-stack time migration possesses peculiar properties, which can lead to a different viewpoint on migration. One of the most interesting properties is an ability to decompose the time migration procedure into a cascade of two or more migrations with smaller migration velocities. This remarkable property is described by Rothman et al. (1985) as *residual migration*. Larner and Beasley (1987) generalized the method of residual migration to one of *cascaded migration*. Cascading finite-difference migrations overcomes the dip limitations of conventional finite-difference algorithms (Larner and Beasley, 1987); cascading Stolt-type *f-k* migrations expands their range of validity to the case of a vertically varying velocity (Beasley et al., 1988). Further theoretical generalization sets the number of migrations in a cascade to infinity, making each step in the velocity space infinitesimally small. This leads to a partial differential equation in the

¹**e-mail:** sergey@sep.stanford.edu

time-midpoint-velocity space, discovered by Claerbout (1986). Claerbout's equation describes the process of *velocity continuation*, which fills the velocity space in the same manner as a set of constant-velocity migrations. Slicing in the migration velocity space can serve as a method of velocity analysis for migration with nonconstant velocity (Shurtleff, 1984; Fowler, 1984, 1988; Mikulich and Hale, 1992).

The concept of velocity continuation was introduced in the earlier publications (Fomel, 1994, 1997). Hubral et al. (1996) and Schleicher et al. (1997) use the term *image waves* to describe a similar idea. Adler (2002) generalizes it to the case of variable background velocities under the name *Kirchhoff image propagation*. The importance of this concept lies in its ability to predict changes in the geometry and intensity of reflection events on seismic images with the change of migration velocity. While conventional approaches to migration velocity analysis methods take into account only vertical movement of reflectors (Deregowski, 1990; Liu and Bleistein, 1995), velocity continuation attempts to describe both vertical and lateral movements, thus providing for optimal focusing in velocity analysis applications (Fomel, 2001, 2003b).

In this paper, I describe the velocity continuation theory for the case of prestack time migration, connecting it with the theory of prestack residual migration (Al-Yahya and Fowler, 1986; Etgen, 1990; Stolt, 1996). By exploiting the mathematical theory of characteristics, a simplified kinematic derivation of the velocity continuation equation leads to a differential equation with correct dynamic properties. In practice, one can accomplish dynamic velocity continuation by integral, finite-difference, or spectral methods. The accompanying paper (Fomel, 2003b) introduces one of the possible numerical implementations and demonstrates its application on a field data example.

The paper is organized into two main sections. First, I derive the kinematics of velocity continuation from the first geometric principles. I identify three distinctive terms, corresponding to zero-offset residual migration, residual normal moveout, and residual dip moveout. Each term is analyzed separately to derive an analytical prediction for the changes in the geometry of traveltime curves (reflection events on migrated images) with the change of migration velocity. Second, the dynamic behavior of seismic images is described with the help of partial differential equations and their solutions. Reconstruction of the dynamical counterparts for kinematic equations is not unique. However, I show that, with an appropriate selection of additional terms, the image waves corresponding to the velocity continuation process have the correct dynamic behavior. In particular, a special boundary value problem with the zero-offset velocity continuation equation produces the solution identical to the conventional Kirchhoff time migration.

KINEMATICS OF VELOCITY CONTINUATION

From the kinematic point of view, it is convenient to describe the reflector as a locally smooth surface $z = z(x)$, where z is the depth, and x is the point on the surface (x is a

two-dimensional vector in the 3-D problem). The image of the reflector obtained after a common-offset prestack migration with a half-offset h and a constant velocity v is the surface $z = z(x; h, v)$. Appendix A provides the derivations of the partial differential equation describing the image surface in the depth-midpoint-offset-velocity space. The purpose of this section is to discuss the laws of kinematic transformations implied by the velocity continuation equation. Later in this paper, I obtain dynamic analogs of the kinematic relationships in order to describe the continuation of migrated sections in the velocity space.

The kinematic equation for prestack velocity continuation, derived in Appendix A, takes the following form:

$$\frac{\partial \tau}{\partial v} = v \tau \left(\frac{\partial \tau}{\partial x} \right)^2 + \frac{h^2}{v^3 \tau} - \frac{h^2 v}{\tau} \left(\frac{\partial \tau}{\partial x} \right)^2 \left(\frac{\partial \tau}{\partial h} \right)^2. \quad (1)$$

Here τ denotes the one-way vertical traveltime ($\tau = \frac{z}{v}$). The right-hand side of equation (1) consists of three distinctive terms. Each has its own geophysical meaning. The first term is the only one remaining when the half-offset h equals zero. This term corresponds to the procedure of *zero-offset residual migration*. Setting the traveltime dip to zero eliminates the first and third terms, leaving the second, dip-independent one. One can associate the second term with the process of *residual normal moveout*. The third term is both dip- and offset- dependent. The process that it describes is *residual dip moveout*. It is convenient to analyze each of the three processes separately, evaluating their contributions to the cumulative process of prestack velocity continuation.

Kinematics of Zero-Offset Velocity Continuation

The kinematic equation for zero-offset velocity continuation is

$$\frac{\partial \tau}{\partial v} = v \tau \left(\frac{\partial \tau}{\partial x} \right)^2. \quad (2)$$

The typical boundary-value problem associated with it is to find the traveltime surface $\tau_2(x_2)$ for a constant velocity v_2 , given the traveltime surface $\tau_1(x_1)$ at some other velocity v_1 . Both surfaces correspond to the reflector images obtained by time migrations with the specified velocities. When the migration velocity approaches zero, post-stack time migration approaches the identity operator. Therefore, the case of $v_1 = 0$ corresponds kinematically to the zero-offset (post-stack) migration, and the case of $v_2 = 0$ corresponds to the zero-offset modeling (demigration). The variable x in equation (2) describes both the surface midpoint coordinate and the subsurface image coordinate. One of them is continuously transformed into the other in the velocity continuation process.

The appropriate mathematical method of solving the kinematic problem posed above is the method of characteristics (Courant and Hilbert, 1989). The characteristics of equation (2) are the trajectories followed by individual points of the reflector

image in the velocity continuation process. These trajectories are called *velocity rays* (Fomel, 1994; Liptow and Hubral, 1995; Adler, 2002). Velocity rays are defined by the system of ordinary differential equations derived from (2) according to the Hamilton-Jacobi theory:

$$\frac{dx}{dv} = -2v\tau\tau_x, \quad \frac{d\tau}{dv} = -\tau_v, \quad (3)$$

$$\frac{d\tau_x}{dv} = v\tau_x^3, \quad \frac{d\tau_v}{dv} = (\tau + v\tau_v)\tau_x^2, \quad (4)$$

where τ_x and τ_v are the phase-space parameters. An additional constraint for τ_x and τ_v follows from equation (2), rewritten in the form

$$\tau_v = v\tau\tau_x^2. \quad (5)$$

The general solution of the system of equations (3-4) takes the parametric form

$$x(v) = A - Cv^2, \quad \tau^2(v) = B - C^2v^2, \quad (6)$$

$$\tau_x(v) = \frac{C}{\tau(v)}, \quad \tau_v(v) = \frac{C^2v}{\tau(v)}, \quad (7)$$

where A , B , and C are constant along each individual velocity ray. These three constants are determined from the boundary conditions as

$$A = x_1 + v_1^2\tau_1 \frac{\partial\tau_1}{\partial x_1} = x_0, \quad (8)$$

$$B = \tau_1^2 \left(1 + v_1^2 \left(\frac{\partial\tau_1}{\partial x_1} \right)^2 \right) = \tau_0^2, \quad (9)$$

$$C = \tau_1 \frac{\partial\tau_1}{\partial x_1} = \tau_0 \frac{\partial\tau_0}{\partial x_0}, \quad (10)$$

where τ_0 and x_0 correspond to the zero velocity (unmigrated section), while τ_1 and x_1 correspond to the velocity v_1 . The simple relationship between the midpoint derivative of the vertical traveltime and the local dip angle α (appendix A),

$$\frac{\partial\tau}{\partial x} = \frac{\tan\alpha}{v}, \quad (11)$$

shows that equations (8) and (9) are precisely equivalent to the evident geometric relationships (Figure 1)

$$x_1 + v_1\tau_1 \tan\alpha = x_0, \quad \frac{\tau_1}{\cos\alpha} = \tau_0. \quad (12)$$

Equation (10) states that the points on a velocity ray correspond to a single reflection point, constrained by the values of τ_1 , v_1 , and α . As follows from equations (6), the projection of a velocity ray to the time-midpoint plane has the parabolic shape $x(\tau) = A + (\tau^2 - B)/C$, which has been noticed by Chun and Jacewitz (1981).

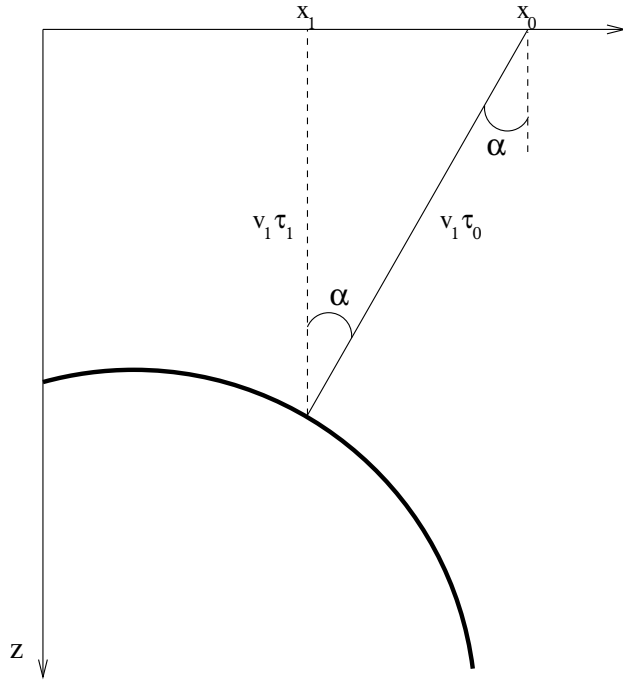


Figure 1: Zero-offset reflection in a constant velocity medium (a scheme).

On the depth-midpoint plane, the velocity rays have the circular shape $z^2(x) = (A - x)B/C - (A - x)^2$, described by Liptow and Hubral (1995) as “Thales circles.”

For an example of kinematic continuation by velocity rays, let us consider the case of a point diffractor. If the diffractor location in the subsurface is the point x_d, z_d , then the reflection traveltime at zero offset is defined from Pythagoras’s theorem as the hyperbolic curve

$$\tau_0(x_0) = \frac{\sqrt{z_d^2 + (x_0 - x_d)^2}}{v_d}, \quad (13)$$

where v_d is half of the actual velocity. Applying equations (6) produces the following mathematical expressions for the velocity rays:

$$x(v) = x_d \frac{v^2}{v_d^2} + x_0 \left(1 - \frac{v^2}{v_d^2}\right), \quad (14)$$

$$\tau^2(v) = \tau_d^2 + \frac{(x_0 - x_d)^2}{v_d^2} \left(1 - \frac{v^2}{v_d^2}\right), \quad (15)$$

where $\tau_d = \frac{z_d}{v_d}$. Eliminating x_0 from the system of equations (14) and (15) leads to the expression for the velocity continuation “wavefront”:

$$\tau(x) = \sqrt{\tau_d^2 + \frac{(x - x_d)^2}{v_d^2 - v^2}}. \quad (16)$$

For the case of a point diffractor, the wavefront corresponds precisely to the summation path of the residual migration operator (Rothman et al., 1985). It has a

hyperbolic shape when $v_d > v$ (undermigration) and an elliptic shape when $v_d < v$ (overmigration). The wavefront collapses to a point when the velocity v approaches the actual effective velocity v_d . At zero velocity, $v = 0$, the wavefront takes the familiar form of the post-stack migration hyperbolic summation path. The form of the velocity rays and wavefronts is illustrated in the left plot of Figure 2.

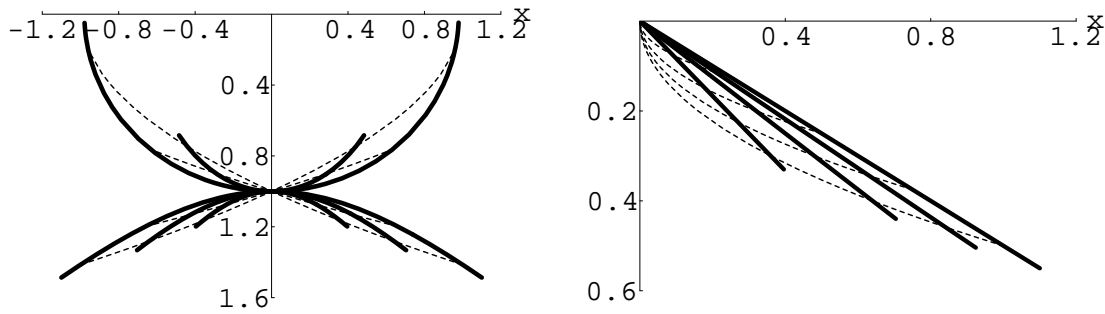


Figure 2: Kinematic velocity continuation in the post-stack migration domain. Solid lines denote wavefronts: reflector images for different migration velocities; dashed lines denote velocity rays. a: the case of a point diffractor. b: the case of a dipping plane reflector.

Another important example is the case of a dipping plane reflector. For simplicity, let us put the origin of the midpoint coordinate x at the point of the plane intersection with the surface of observations. In this case, the depth of the plane reflector corresponding to the surface point x has the simple expression

$$z_p(x) = x \tan \alpha , \quad (17)$$

where α is the dip angle. The zero-offset reflection traveltime $\tau_0(x_0)$ is the plane with a changed angle. It can be expressed as

$$\tau_0(x_0) = p x_0 , \quad (18)$$

where $p = \frac{\sin \alpha}{v_p}$, and v_p is half of the actual velocity. Applying formulas (6) leads to the following parametric expression for the velocity rays:

$$x(v) = x_0 (1 - p^2 v^2) , \quad (19)$$

$$\tau(v) = p x_0 \sqrt{1 - p^2 v^2} . \quad (20)$$

Eliminating x_0 from the system of equations (19) and (20) shows that the velocity continuation wavefronts are planes with a modified angle:

$$\tau(x) = \frac{p x}{\sqrt{1 - p^2 v^2}} . \quad (21)$$

The right plot of Figure 2 shows the geometry of the kinematic velocity continuation for the case of a plane reflector.

Kinematics of Residual NMO

The residual NMO differential equation is the second term in equation (1):

$$\frac{\partial \tau}{\partial v} = \frac{h^2}{v^3 \tau}. \quad (22)$$

Equation (22) does not depend on the midpoint x . This fact indicates the one-dimensional nature of normal moveout. The general solution of equation (22) is obtained by simple integration. It takes the form

$$\tau^2(v) = C - \frac{h^2}{v^2} = \tau_1^2 + h^2 \left(\frac{1}{v_1^2} - \frac{1}{v^2} \right), \quad (23)$$

where C is an arbitrary velocity-independent constant, and I have chosen the constants τ_1 and v_1 so that $\tau(v_1) = \tau_1$. Equation (23) is applicable only for v different from zero.

For the case of a point diffractor, equation (23) easily combines with the zero-offset solution (16). The result is a simplified approximate version of the prestack residual migration summation path:

$$\tau(x) = \sqrt{\tau_d^2 + \frac{(x - x_d)^2}{v_d^2 - v^2} + h^2 \left(\frac{1}{v_d^2} - \frac{1}{v^2} \right)}. \quad (24)$$

Summation paths of the form (24) for a set of diffractors with different depths are plotted in Figures 3 and 4. The parameters chosen in these plots allow a direct comparison with Etgen's Figures 2.4 and 2.5 (Etgen, 1990), based on the exact solution and reproduced in Figures 8 and 9. The comparison shows that the approximate solution (24) captures the main features of the prestack residual migration operator, except for the residual DMO cusps appearing in the exact solution when the diffractor depth is smaller than the offset.

Neglecting the residual DMO term in residual migration is approximately equivalent in accuracy to neglecting the DMO step in conventional processing. Indeed, as follows from the geometric analog of equation (1) derived in Appendix A [equation (A-17)], dropping the residual DMO term corresponds to the condition

$$\tan^2 \alpha \tan^2 \theta \ll 1, \quad (25)$$

where α is the dip angle, and θ is the reflection angle. As shown by Yilmaz and Claerbout (1980), the conventional processing sequence without the DMO step corresponds to the separable approximation of the double-square-root equation (A-4):

$$\sqrt{1 - v^2 \left(\frac{\partial t}{\partial s} \right)^2} + \sqrt{1 - v^2 \left(\frac{\partial t}{\partial r} \right)^2} \approx 2 \sqrt{1 - v^2 \left(\frac{\partial t}{\partial x} \right)^2} + 2 \sqrt{1 - v^2 \left(\frac{\partial t}{\partial h} \right)^2} - 2, \quad (26)$$

Figure 3: Summation paths of the simplified prestack residual migration for a series of depth diffractors. Residual slowness v/v_d is 1.2; half-offset h is 1 km. This figure is to be compared with Etgen's Figure 2.4, reproduced in Figure 8.

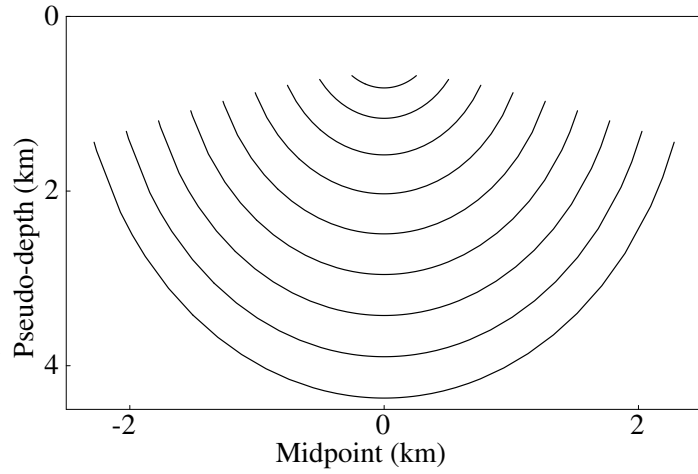
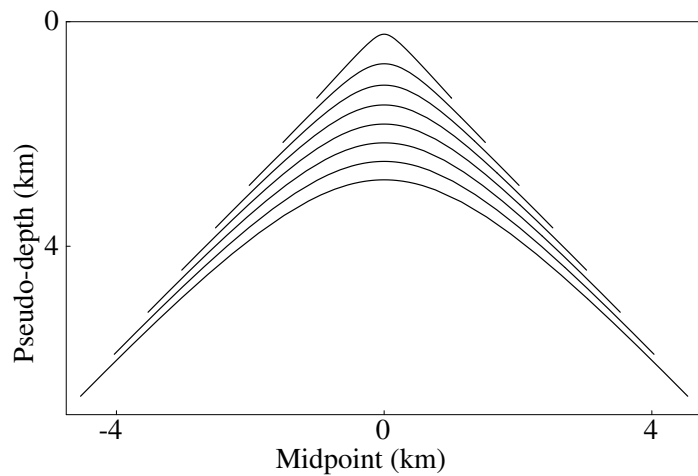


Figure 4: Summation paths of the simplified prestack residual migration for a series of depth diffractors. Residual slowness v/v_d is 0.8; offset h is 1 km. This figure is to be compared with Etgen's Figure 2.5, reproduced in Figure 9.



where t is the reflection traveltime, and s and r are the source and receiver coordinates: $s = x - h$, $r = x + h$. In geometric terms, approximation (26) transforms to

$$\cos \alpha \cos \theta \approx \sqrt{1 - \sin^2 \alpha \cos^2 \theta} + \sqrt{1 - \sin^2 \theta \cos^2 \alpha} - 1. \quad (27)$$

Taking the difference of the two sides of equation (27), one can estimate its accuracy by the first term of the Taylor series for small α and θ . The estimate is $\frac{3}{4} \tan^2 \alpha \tan^2 \theta$ (Yilmaz and Claerbout, 1980), which agrees qualitatively with (25). Although approximation (24) fails in situations where the dip moveout correction is necessary, it is significantly more accurate than the 15-degree approximation of the double-square-root equation, implied in the migration velocity analysis method of Yilmaz and Chambers (1984) and MacKay and Abma (1992). The 15-degree approximation

$$\sqrt{1 - v^2 \left(\frac{\partial t}{\partial s}\right)^2} + \sqrt{1 - v^2 \left(\frac{\partial t}{\partial r}\right)^2} \approx 2 - \frac{v^2}{2} \left(\left(\frac{\partial t}{\partial s}\right)^2 + \left(\frac{\partial t}{\partial r}\right)^2 \right) \quad (28)$$

corresponds geometrically to the equation

$$2 \cos \alpha \cos \theta \approx \frac{3 + \cos 2\alpha \cos 2\theta}{2}. \quad (29)$$

Its estimated accuracy (from the first term of the Taylor series) is $\frac{1}{8} \tan^2 \alpha + \frac{1}{8} \tan^2 \theta$. Unlike the separable approximation, which is accurate separately for zero offset and zero dip, the 15-degree approximation fails at zero offset in the case of a steep dip and at zero dip in the case of a large offset.

Kinematics of Residual DMO

The partial differential equation for kinematic residual DMO is the third term in equation (1):

$$\frac{\partial \tau}{\partial v} = -\frac{h^2 v}{\tau} \left(\frac{\partial \tau}{\partial x}\right)^2 \left(\frac{\partial \tau}{\partial h}\right)^2. \quad (30)$$

It is more convenient to consider the residual dip-moveout process coupled with residual normal moveout. Etgen (1990) describes this procedure as the cascade of inverse DMO with the initial velocity v_0 , residual NMO, and DMO with the updated velocity v_1 . The kinematic equation for residual NMO+DMO is the sum of the two terms in (1):

$$\frac{\partial \tau}{\partial v} = \frac{h^2}{v^3 \tau} \left(1 - v^4 \left(\frac{\partial \tau}{\partial x}\right)^2 \left(\frac{\partial \tau}{\partial h}\right)^2 \right). \quad (31)$$

The derivation of the residual DMO+NMO kinematics is detailed in Appendix B. Figure 5 illustrates it with the theoretical impulse response curves. Figure 6 compares the theoretical curves with the result of an actual cascade of the inverse DMO, residual NMO, and DMO operators.

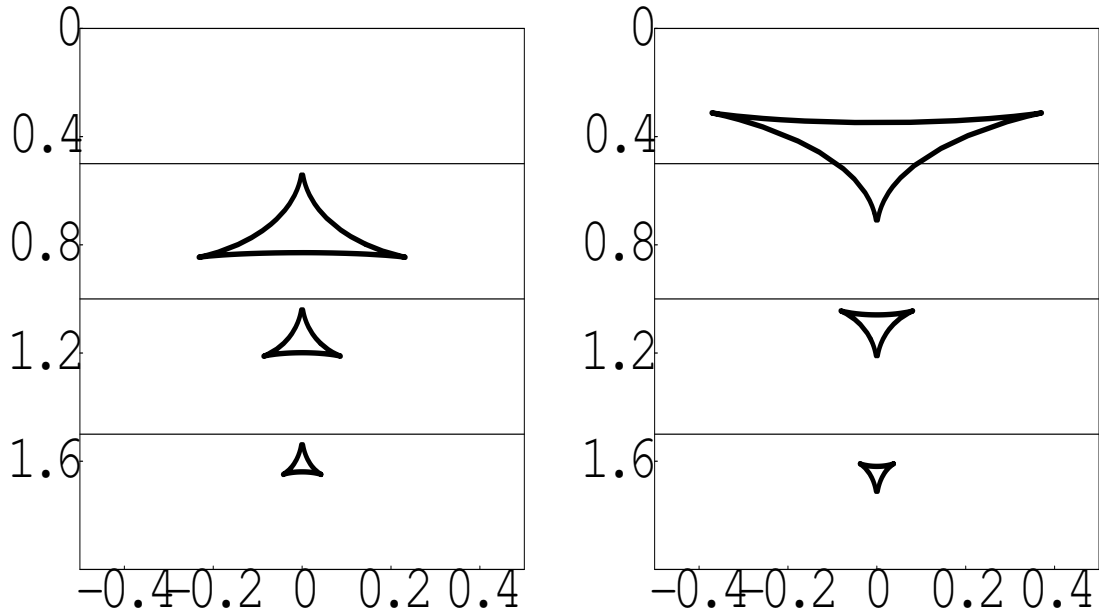


Figure 5: Theoretical kinematics of the residual NMO+DMO impulse responses for three impulses. Left plot: the velocity ratio v_1/v_0 is 1.333. Right plot: the velocity ratio v_1/v_0 is 0.833. In both cases the half-offset h is 1 km.

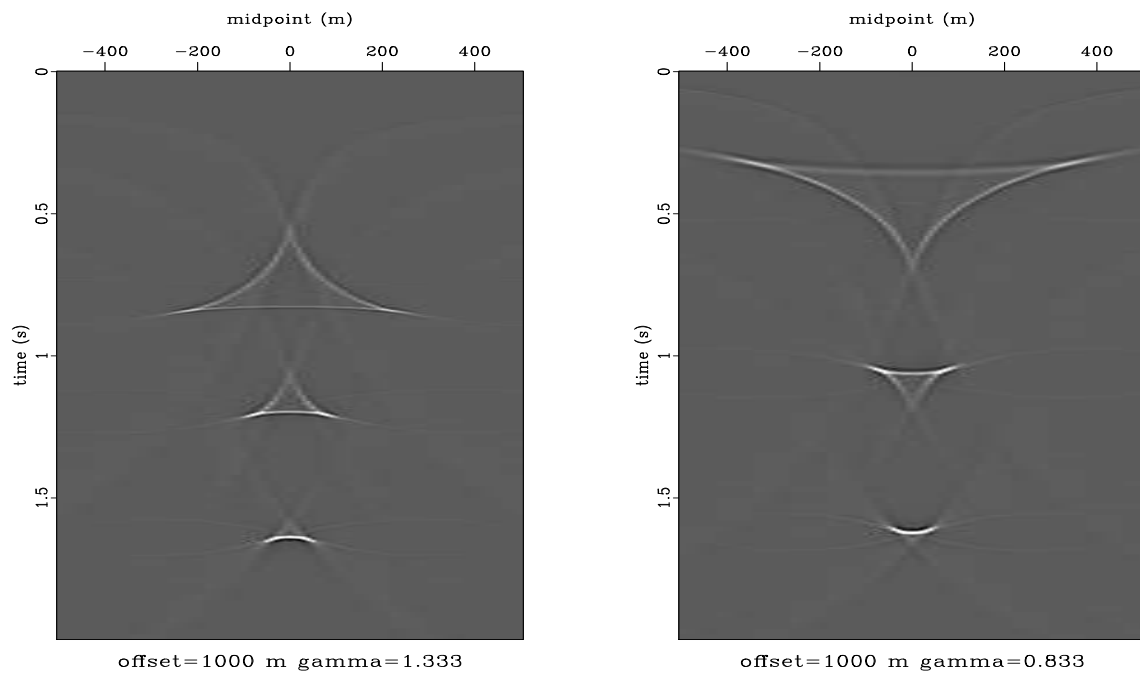


Figure 6: The result of residual NMO+DMO (cascading inverse DMO, residual NMO, and DMO) for three impulses. Left plot: the velocity ratio v_1/v_0 is 1.333. Right plot: the velocity ratio v_1/v_0 is 0.833. In both cases the half-offset h is 1 km.

Figure 7 illustrates the residual NMO+DMO velocity continuation for two particularly interesting cases. The left plot shows the continuation for a point diffractor. One can see that when the velocity error is large, focusing of the velocity rays forms a distinctive loop on the zero-offset hyperbola. The right plot illustrates the case of a plane dipping reflector. The image of the reflector shifts both vertically and laterally with the change in NMO velocity.

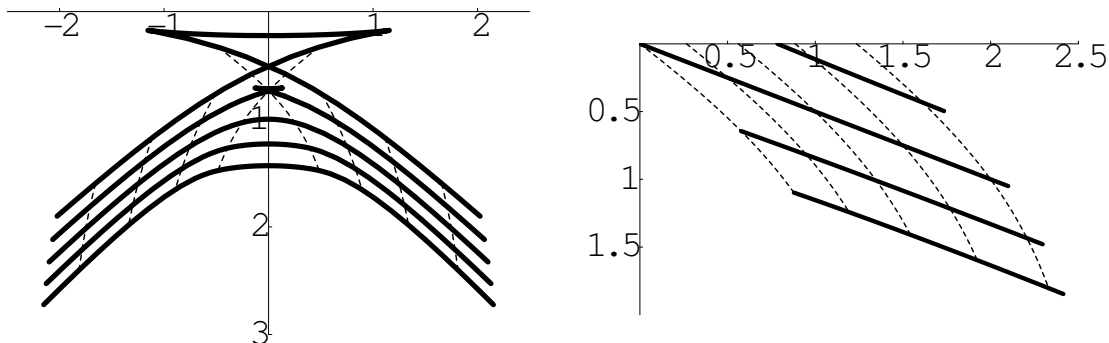


Figure 7: Kinematic velocity continuation for residual NMO+DMO. Solid lines denote wavefronts: zero-offset travelttime curves; dashed lines denote velocity rays. a: the case of a point diffractor; the velocity ratio v_1/v_0 changes from 0.9 to 1.1. b: the case of a dipping plane reflector; the velocity ratio v_1/v_0 changes from 0.8 to 1.2. In both cases, the half-offset h is 2 km.

The full residual migration operator is the chain of residual zero-offset migration and residual NMO+DMO. I illustrate the kinematics of this operator in Figures 8 and 9, which are designed to match Etgen's Figures 2.4 and 2.5 (Etgen, 1990). A comparison with Figures 3 and 4 shows that including the residual DMO term affects the images of objects with the depth smaller than the half-offset h . This term complicates the residual migration operator with cusps.

FROM KINEMATICS TO DYNAMICS

The theory of characteristics (Courant and Hilbert, 1989) states that if a partial differential equation has the form

$$\sum_{i,j=1}^n \Lambda_{ij}(\xi_1, \dots, \xi_n) \frac{\partial^2 P}{\partial \xi_i \partial \xi_j} + F\left(\xi_1, \dots, \xi_n, P, \frac{\partial P}{\partial \xi_1}, \dots, \frac{\partial P}{\partial \xi_n}\right) = 0, \quad (32)$$

where F is some arbitrary function, and if the eigenvalues of the matrix Λ are nonzero, and one of them is different in sign from the others, then equation (32) describes a

Figure 8: Summation paths of prestack residual migration for a series of depth diffractors. Residual slowness v/v_d is 1.2; half-offset h is 1 km. This figure reproduces Etgen's Figure 2.4.

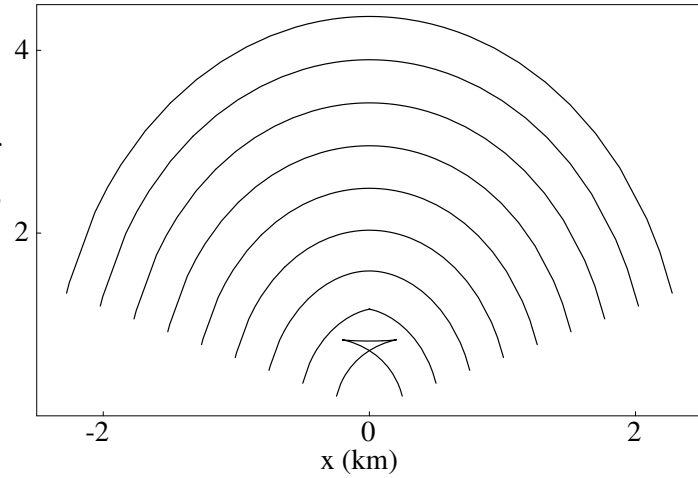
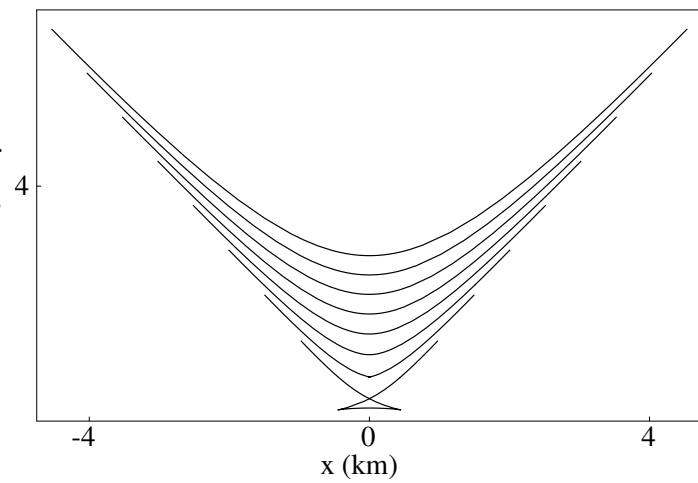


Figure 9: Summation paths of prestack residual migration for a series of depth diffractors. Residual slowness v/v_d is 0.8; half-offset h is 1 km. This figure reproduces Etgen's Figure 2.5.



wave-type process, and its kinematic counterpart is the characteristic equation

$$\sum_{i,j=1}^n \Lambda_{ij}(\xi_1, \dots, \xi_n) \frac{\partial \psi}{\partial \xi_i} \frac{\partial \psi}{\partial \xi_j} = 0 \quad (33)$$

with the characteristic surface

$$\psi(\xi_1, \dots, \xi_n) = 0 \quad (34)$$

corresponding to the wavefront. In velocity continuation problems, it is appropriate to choose the variable ξ_1 to denote the time t , ξ_2 to denote the velocity v , and the rest of the ξ -variables to denote one or two lateral coordinates x . Without loss of generality, let us set the characteristic surface to be

$$\psi = t - \tau(x; v) = 0, \quad (35)$$

and use the theory of characteristics to reconstruct the main (second-order) part of the dynamic differential equation from the corresponding kinematic equations. As in the preceding section, it is convenient to consider separately the three different components of the prestack velocity continuation process.

Dynamics of Zero-Offset Velocity Continuation

In the case of zero-offset velocity continuation, the characteristic equation is reconstructed from equation (2) to have the form

$$\frac{\partial \psi}{\partial v} \frac{\partial \psi}{\partial t} + v t \left(\frac{\partial \psi}{\partial x} \right)^2 = 0, \quad (36)$$

where τ is replaced by t according to equation (35). According to equation (32), the corresponding dynamic equation is

$$\frac{\partial^2 P}{\partial v \partial t} + v t \frac{\partial^2 P}{\partial x^2} + F \left(x, t, v, P, \frac{\partial P}{\partial t}, \frac{\partial P}{\partial v}, \frac{\partial P}{\partial x} \right) = 0, \quad (37)$$

where the function F remains to be defined. The simplest case of F equal to zero corresponds to Claerbout's velocity continuation equation (Claerbout, 1986), derived in a different way. Levin (1986a) provides the dispersion-relation derivation, conceptually analogous to applying the method of characteristics.

In high-frequency asymptotics, the wavefield P can be represented by the ray-theoretical (WKBJ) approximation,

$$P(t, x, v) \approx A(x, v) f(t - \tau(x, v)), \quad (38)$$

where A is the amplitude, f is the short (high-frequency) wavelet, and the function τ satisfies the kinematic equation (2). Substituting approximation (38) into

the dynamic velocity continuation equation (37), collecting the leading-order terms, and neglecting the F function leads to the partial differential equation for amplitude transport:

$$\frac{\partial A}{\partial v} = v \tau \left(2 \frac{\partial A}{\partial x} \frac{\partial \tau}{\partial x} + A \frac{\partial^2 \tau}{\partial x^2} \right). \quad (39)$$

The general solution of equation (39) follows from the theory of characteristics. It takes the form

$$A(x, v) = A(x_0, 0) \exp \left(\int_0^v u \tau(x, u) \frac{\partial^2 \tau(x, u)}{\partial x^2} du \right), \quad (40)$$

where the integral corresponds to the curvilinear integration along the corresponding velocity ray, and x_0 corresponds to the starting point of the ray. In the case of a plane dipping reflector, the image of the reflector remains plane in the velocity continuation process. Therefore, the second travelttime derivative $\frac{\partial^2 \tau(x, u)}{\partial x^2}$ in (40) equals zero, and the exponential is equal to one. This means that the amplitude of the image does not change with the velocity along the velocity rays. This fact does not agree with the theory of conventional post-stack migration, which suggests downscaling the image by the ‘‘cosine’’ factor $\frac{v_0}{v}$ (Chun and Jacewitz, 1981; Levin, 1986b). The simplest way to include the cosine factor in the velocity continuation equation is to set the function F to be $\frac{1}{t} \frac{\partial P}{\partial v}$. The resulting differential equation

$$\frac{\partial^2 P}{\partial v \partial t} + v t \frac{\partial^2 P}{\partial x^2} + \frac{1}{t} \frac{\partial P}{\partial v} = 0 \quad (41)$$

has the amplitude transport

$$A(x, v) = \frac{\tau_0}{\tau} A(x_0, 0) \exp \left(\int_0^v u \tau(x, u) \frac{\partial^2 \tau(x, u)}{\partial x^2} du \right), \quad (42)$$

corresponding to the differential equation

$$\frac{\partial A}{\partial v} = v \tau \left(2 \frac{\partial A}{\partial x} \frac{\partial \tau}{\partial x} + A \frac{\partial^2 \tau}{\partial x^2} \right) - A \frac{1}{\tau} \frac{\partial \tau}{\partial v}. \quad (43)$$

Appendix C proves that the time-and-space solution of the dynamic velocity continuation equation (41) coincides with the conventional Kirchhoff migration operator.

Dynamics of Residual NMO

According to the theory of characteristics, described in the beginning of this section, the kinematic residual NMO equation (22) corresponds to the dynamic equation of the form

$$\frac{\partial P}{\partial v} + \frac{h^2}{v^3 t} \frac{\partial P}{\partial t} + F(h, t, v, P) = 0 \quad (44)$$

with the undetermined function F . In the case of $F = 0$, the general solution is easily found to be

$$P(t, h, v) = \phi \left(t^2 + \frac{h^2}{v^2} \right). \quad (45)$$

where ϕ is an arbitrary smooth function. The combination of dynamic equations (44) and (41) leads to an approximate prestack velocity continuation with the residual DMO effect neglected. To accomplish the combination, one can simply add the term $\frac{h^2}{v^3 t} \frac{\partial^2 P}{\partial t^2}$ from equation (44) to the left-hand side of equation (41). This addition changes the kinematics of velocity continuation, but does not change the amplitude properties embedded in the transport equation (42).

Dunkin and Levin (1973) and Hale (1983) advocate using an amplitude correction term in the NMO step. This term can be easily added by selecting an appropriate function F in equation (44). The choice $F = \frac{h^2}{v^3 t^2} P$ results in the equation

$$\frac{\partial P}{\partial v} + \frac{h^2}{v^3 t^2} \left(t \frac{\partial P}{\partial t} + P \right) = 0 \quad (46)$$

with the general solution

$$P(t, h, v) = \frac{1}{t} \phi \left(t^2 + \frac{h^2}{v^2} \right), \quad (47)$$

which has the Dunkin-Levin amplitude correction term.

Dynamics of Residual DMO

The case of residual DMO complicates the building of a dynamic equation because of the essential nonlinearity of the kinematic equation (30). One possible way to linearize the problem is to increase the order of the equation. In this case, the resultant dynamic equation would include a term that has the second-order derivative with respect to velocity v . Such an equation describes two different modes of wave propagation and requires additional initial conditions to separate them. Another possible way to linearize equation (30) is to approximate it at small dip angles. In this case, the dynamic equation would contain only the first-order derivative with respect to the velocity and high-order derivatives with respect to the other parameters. The third, and probably the most attractive, method is to change the domain of consideration. For example, one could switch from the common-offset domain to the domain of offset dip. This method implies a transformation similar to slant stacking of common-midpoint gathers in the post-migration domain in order to obtain the local offset dip information. Equation (30) transforms, with the help of the results from Appendix A, to the form

$$v^3 \frac{\partial \tau}{\partial v} = \frac{\tau \sin^2 \theta}{\cos^2 \alpha - \sin^2 \theta}, \quad (48)$$

with

$$\cos^2 \alpha = \left(1 + v^2 \left(\frac{\partial \tau}{\partial x} \right)^2 \right)^{-1}, \quad (49)$$

and

$$\sin^2 \alpha = v^2 \left(\frac{\partial \tau}{\partial h} \right)^2 \left(1 + v^2 \left(\frac{\partial \tau}{\partial h} \right)^2 \right)^{-1}. \quad (50)$$

For a constant offset dip $\tan \theta = v \frac{\partial \tau}{\partial h}$, the dynamic analog of equation (48) is the third-order partial differential equation

$$v \cot^2 \theta \frac{\partial^3 P}{\partial t^2 \partial v} - v^3 \frac{\partial^3 P}{\partial x^2 \partial v} + t \frac{\partial^3 P}{\partial t^2 \partial v} + v^2 t \frac{\partial^3 P}{\partial x^2 \partial t} = 0. \quad (51)$$

Equation (51) does not strictly comply with the theory of second-order linear differential equations. Its properties and practical applicability require further research.

CONCLUSIONS

I have derived kinematic and dynamic equations for residual time migration in the form of a continuous velocity continuation process. This derivation explicitly decomposes prestack velocity continuation into three parts corresponding to zero-offset continuation, residual NMO, and residual DMO. These three parts can be treated separately both for simplicity of theoretical analysis and for practical purposes. It is important to note that in the case of a three-dimensional migration, all three components of velocity continuation have different dimensionality. Zero-offset continuation is fully 3-D. It can be split into two 2-D continuations in the in- and cross-line directions. Residual DMO is a two-dimensional common-azimuth process. Residual NMO is a 1-D single-trace procedure.

The dynamic properties of zero-offset velocity continuation are precisely equivalent to those of conventional post-stack migration methods such as Kirchhoff migration. Moreover, the Kirchhoff migration operator coincides with the integral solution of the velocity continuation differential equation for continuation from the zero velocity plane.

This rigorous theory of velocity continuation gives us new insights into the methods of prestack migration velocity analysis. Extensions to the case of depth migration in a variable velocity background are developed by Liu and McMechan (1996) and Adler (2002). A practical application of velocity continuation to migration velocity analysis is demonstrated in the companion paper (Fomel, 2003b), where the general theory is used to design efficient and practical algorithms.

ACKNOWLEDGMENTS

This work was completed when the author was a member of the Stanford Exploration Project (SEP) at Stanford University. The financial support was provided by the SEP sponsors.

I thank Bee Bednar, Biondo Biondi, Jon Claerbout, Sergey Goldin, Bill Harlan, David Lumley, and Bill Symes for useful and stimulating discussions. Paul Fowler, Hugh Geiger, Samuel Gray, and one anonymous reviewer provided valuable suggestions that improved the quality of the paper.

REFERENCES

- Adler, F., 2002, Kirchhoff image propagation: *Geophysics*, **67**, 126–134.
- Al-Yahya, K., and P. Fowler, 1986, Prestack residual migration, *in* SEP-50: Stanford Exploration Project, 219–230.
- Beasley, C., W. Lynn, K. Larner, and H. Nguyen, 1988, Cascaded frequency-wavenumber migration - Removing the restrictions on depth-varying velocity: *Geophysics*, **53**, 881–893.
- Belonosova, A. V., and A. S. Alekseev, 1967, *in* About one formulation of the inverse kinematic problem of seismics for a two-dimensional continuously heterogeneous medium: Nauka, 137–154.
- Berkhout, A. J., 1985, Seismic migration: Imaging of acoustic energy by wave field extrapolation: Elsevier, Amsterdam.
- Chun, J. H., and C. A. Jacewitz, 1981, Fundamentals of frequency-domain migration: *Geophysics*, **46**, 717–733.
- Claerbout, J. F., 1985, *Imaging the Earth's Interior*: Blackwell Scientific Publications.
- , 1986, Velocity extrapolation by cascaded 15 degree migration, *in* SEP-48: Stanford Exploration Project, 79–84.
- Clayton, R. W., 1978, Common midpoint migration, *in* SEP-14: Stanford Exploration Project, 21–36.
- Courant, R., and D. Hilbert, 1989, *Methods of mathematical physics*: John Wiley & Sons.
- Deregowski, S. M., 1990, Common-offset migrations and velocity analysis: *First Break*, **08**, 224–234.
- Dunkin, J. W., and F. K. Levin, 1973, Effect of normal moveout on a seismic pulse: *Geophysics*, **38**, 635–642.
- Etgen, J., 1990, Residual prestack migration and interval velocity estimation: PhD thesis, Stanford University.
- Fomel, S., 1997, Velocity continuation and the anatomy of prestack residual migration: 67th Ann. Internat. Mtg, Soc. of Expl. Geophys., 1762–1765.
- , 2001, Migration velocity analysis by velocity continuation: 71st Ann. Internat. Mtg, Soc. of Expl. Geophys., 1107–1110.
- , 2003a, Theory of differential offset continuation: *Geophysics*, in press.

- , 2003b, Time migration velocity analysis by velocity continuation: Geophysics, submitted for publication.
- Fomel, S. B., 1994, Method of velocity continuation in the problem of temporal seismic migration: *Russian Geology and Geophysics*, **35**, 100–111.
- Fowler, P., 1984, Velocity independent imaging of seismic reflectors: 54th Ann. Internat. Mtg. Soc. of Expl. Geophys., Session:S1.8.
- , 1988, Seismic velocity estimation using prestack time migration: PhD thesis, Stanford University.
- Gradshteyn, I. S., and I. M. Ryzhik, 1994, Table of integrals, series, and products: Boston: Academic Press.
- Hale, I. D., 1983, Dip moveout by Fourier transform: PhD thesis, Stanford University.
- Hubral, P., M. Tygel, and J. Schleicher, 1996, Seismic image waves: *Geophysical Journal International*, **125**, 431–442.
- Jakubowicz, H., and S. Levin, 1983, A simple exact method of three-dimensional migration - Theory: *Geophys. Prosp.*, **31**, 34–56. (Discussion in GPR-34-06-0927-0939 with reply by author; Comment in GPR-32-02-0347-0350 with reply by author).
- Larner, K., and C. Beasley, 1987, Cascaded migrations - Improving the accuracy of finite-difference migration: *Geophysics*, **52**, 618–643. (Errata in GEO-52-8-1165).
- Levin, S., 1986a, Cascaded fifteen degree equations simplified, *in* SEP-48: Stanford Exploration Project, 101–108.
- , 1986b, Test your migration IQ, *in* SEP-48: Stanford Exploration Project, 147–160.
- Liptow, F., and P. Hubral, 1995, Migrating around in circles: *The Leading Edge*, **14**, 1125–1127.
- Liu, H., and G. McMechan, 1996, Dynamic residual prestack depth migration for common offset gathers: UTD Report.
- Liu, Z., and N. Bleistein, 1995, Migration velocity analysis: Theory and an iterative algorithm: *Geophysics*, **60**, 142–153.
- MacKay, S., and R. Abma, 1992, Imaging and velocity estimation with depth-focusing analysis: *Geophysics*, **57**, 1608–1622.
- Mikulich, W., and D. Hale, 1992, Steep-dip $v(z)$ imaging from an ensemble of Stolt-like migrations: *Geophysics*, **57**, 51–59.
- Popovici, A. M., 1995, Prestack migration by split-step DSR, *in* SEP-84: Stanford Exploration Project, 53–60.
- Rothman, D. H., S. A. Levin, and F. Rocca, 1985, Residual migration - Applications and limitations: *Geophysics*, **50**, 110–126.
- Sava, P., and S. Fomel, 2003, Wave-equation angle-domain common-image gathers: *Geophysics*, in press.
- Schleicher, J., P. Hubral, G. Hocht, and F. Liptow, 1997, Seismic constant-velocity remigration: *Geophysics*, **62**, 589–597.
- Schneider, W. A., 1978, Integral formulation for migration in two-dimensions and three-dimensions: *Geophysics*, **43**, 49–76.
- Shurtleff, R. N., 1984, An F-K procedure for prestack migration and migration velocity analysis, *in* Presented at the 46th Annual EAGE Mtg., London: EAGE.
- Stolt, R. H., 1978, Migration by Fourier transform: *Geophysics*, **43**, 23–48. (Discus-

- sion and reply in GEO-60-5-1583).
- , 1996, Short note - A prestack residual time migration operator: *Geophysics*, **61**, 605–607.
- Tygel, M., J. Schleicher, and P. Hubral, 1994, Pulse distortion in depth migration: *Geophysics*, **59**, 1561–1569.
- Yilmaz, O., 1979, Prestack partial migration: PhD thesis, Stanford University.
- Yilmaz, O., and R. E. Chambers, 1984, Migration velocity analysis by wave-field extrapolation: *Geophysics*, **49**, 1664–1674.
- Yilmaz, O., and J. F. Claerbout, 1980, Prestack partial migration: *Geophysics*, **45**, 1753–1779.

APPENDIX A

DERIVING THE KINEMATIC EQUATIONS

The main goal of this appendix is to derive the partial differential equation describing the image surface in a depth-midpoint-offset-velocity space.

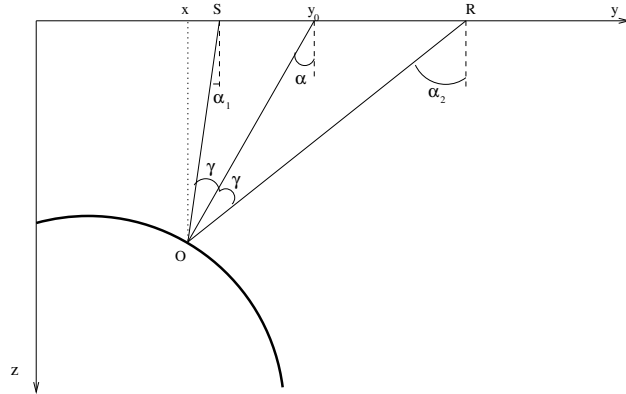


Figure A-1: Reflection rays in a constant velocity medium (a scheme).

The derivation starts with observing a simple geometry of reflection in a constant-velocity medium, shown in Figure A-1. The well-known equations for the apparent slowness

$$\frac{\partial t}{\partial s} = \frac{\sin \alpha_1}{v}, \quad (\text{A-1})$$

$$\frac{\partial t}{\partial r} = \frac{\sin \alpha_2}{v} \quad (\text{A-2})$$

relate the first-order traveltimes derivatives for the reflected waves to the emergence angles of the incident and reflected rays. Here s stands for the source location at the surface, r is the receiver location, t is the reflection traveltimes, v is the constant velocity, and α_1 and α_2 are the angles shown in Figure A-1. Considering the traveltimes derivative with respect to the depth of the observation surface z shows that

the contributions of the two branches of the reflected ray, added together, form the equation

$$-\frac{\partial t}{\partial z} = \frac{\cos \alpha_1}{v} + \frac{\cos \alpha_2}{v}. \quad (\text{A-3})$$

It is worth mentioning that the elimination of angles from equations (A-1), (A-2), and (A-3) leads to the famous *double-square-root equation*,

$$-v \frac{\partial t}{\partial z} = \sqrt{1 - v^2 \left(\frac{\partial t}{\partial s} \right)^2} + \sqrt{1 - v^2 \left(\frac{\partial t}{\partial r} \right)^2}, \quad (\text{A-4})$$

published in the Russian literature by Belonosova and Alekseev (1967) and commonly used in the form of a pseudo-differential dispersion relation (Clayton, 1978; Claerbout, 1985) for prestack migration (Yilmaz, 1979; Popovici, 1995). Considered locally, equation (A-4) is independent of the constant velocity assumption and enables recursive prestack downward continuation of reflected waves in heterogeneous isotropic media.

Introducing the midpoint coordinate $x = \frac{s+r}{2}$ and half-offset $h = \frac{r-s}{2}$, one can apply the chain rule and elementary trigonometric equalities to formulas (A-1) and (A-2) and transform these formulas to

$$\frac{\partial t}{\partial x} = \frac{\partial t}{\partial s} + \frac{\partial t}{\partial r} = \frac{2 \sin \alpha \cos \theta}{v}, \quad (\text{A-5})$$

$$\frac{\partial t}{\partial h} = \frac{\partial t}{\partial r} - \frac{\partial t}{\partial s} = \frac{2 \cos \alpha \sin \theta}{v}, \quad (\text{A-6})$$

where $\alpha = \frac{\alpha_1 + \alpha_2}{2}$ is the dip angle, and $\theta = \frac{\alpha_2 - \alpha_1}{2}$ is the reflection angle (Clayton, 1978; Claerbout, 1985). Equation (A-3) transforms analogously to

$$-\frac{\partial t}{\partial z} = \frac{2 \cos \alpha \cos \theta}{v}. \quad (\text{A-7})$$

This form of equation (A-3) is used to describe the stretching factor of the waveform distortion in depth migration (Tygel et al., 1994).

Dividing (A-5) and (A-6) by (A-7) leads to

$$\frac{\partial z}{\partial x} = -\tan \alpha, \quad (\text{A-8})$$

$$\frac{\partial z}{\partial h} = -\tan \theta. \quad (\text{A-9})$$

Equation (A-9) is the basis of the angle-gather construction of Sava and Fomel (2003). Substituting formulas (A-8) and (A-9) into equation (A-7) yields yet another form of the double-square-root equation:

$$-\frac{\partial t}{\partial z} = \frac{2}{v} \left[\sqrt{1 + \left(\frac{\partial z}{\partial x} \right)^2} \sqrt{1 + \left(\frac{\partial z}{\partial h} \right)^2} \right]^{-1}, \quad (\text{A-10})$$

which is analogous to the dispersion relationship of Stolt prestack migration (Stolt, 1978).

The law of sines in the triangle formed by the incident and reflected ray leads to the explicit relationship between the traveltime and the offset:

$$vt = 2h \frac{\cos \alpha_1 + \cos \alpha_2}{\sin(\alpha_2 - \alpha_1)} = 2h \frac{\cos \alpha}{\sin \theta}. \quad (\text{A-11})$$

An algebraic combination of formulas (A-11), (A-5), and (A-6) forms the basic kinematic equation of the offset continuation theory (Fomel, 2003a):

$$\frac{\partial t}{\partial h} \left(t^2 + \frac{4h^2}{v^2} \right) = ht \left(\frac{4}{v^2} + \left(\frac{\partial t}{\partial h} \right)^2 - \left(\frac{\partial t}{\partial x} \right)^2 \right). \quad (\text{A-12})$$

Differentiating (A-11) with respect to the velocity v yields

$$-v^2 \frac{\partial t}{\partial v} = 2h \frac{\cos \alpha}{\sin \theta}. \quad (\text{A-13})$$

Finally, dividing (A-13) by (A-7) produces

$$v \frac{\partial z}{\partial v} = \frac{h}{\cos \theta \sin \theta}. \quad (\text{A-14})$$

Equation (A-14) can be written in a variety of ways with the help of an explicit geometric relationship between the half-offset h and the depth z ,

$$h = z \frac{\sin \theta \cos \theta}{\cos^2 \alpha - \sin^2 \theta}, \quad (\text{A-15})$$

which follows directly from the trigonometry of the triangle in Figure A-1 (Fomel, 2003a). For example, equation (A-14) can be transformed to the form obtained by Liu and Bleistein (1995):

$$v \frac{\partial z}{\partial v} = \frac{z}{\cos^2 \alpha - \sin^2 \theta} = \frac{z}{\cos \alpha_1 \cos \alpha_2}. \quad (\text{A-16})$$

In order to separate different factors contributing to the velocity continuation process, one can transform this equation to the form

$$\begin{aligned} v \frac{\partial z}{\partial v} &= \frac{z}{\cos^2 \alpha} + \frac{h^2}{z} \left(1 - \tan^2 \alpha \tan^2 \theta \right) \\ &= z \left(1 + \left(\frac{\partial z}{\partial x} \right)^2 \right) + \frac{h^2}{z} \left(1 - \left(\frac{\partial z}{\partial x} \right)^2 \left(\frac{\partial z}{\partial h} \right)^2 \right). \end{aligned} \quad (\text{A-17})$$

Rewritten in terms of the vertical traveltime $\tau = z/v$, it further transforms to equation

$$\frac{\partial \tau}{\partial v} = v \tau \left(\frac{\partial \tau}{\partial x} \right)^2 + \frac{h^2}{v^3 \tau} \left(1 - v^4 \left(\frac{\partial \tau}{\partial x} \right)^2 \left(\frac{\partial \tau}{\partial h} \right)^2 \right), \quad (\text{A-18})$$

equivalent to equation (1) in the main text. Yet another form of the kinematic velocity continuation equation follows from eliminating the reflection angle θ from equations (A-14) and (A-15). The resultant expression takes the following form:

$$v \frac{\partial z}{\partial v} = \frac{2(z^2 + h^2)}{\sqrt{z^2 + h^2 \sin^2 2\alpha} + z \cos 2\alpha} = \frac{z}{\cos^2 \alpha} + \frac{2h^2}{\sqrt{z^2 + h^2 \sin^2 2\alpha} + z}. \quad (\text{A-19})$$

APPENDIX B

DERIVATION OF THE RESIDUAL DMO KINEMATICS

This appendix derives the kinematical laws for the residual NMO+DMO transformation in the prestack offset continuation process.

The direct solution of equation (31) is nontrivial. A simpler way to obtain this solution is to decompose residual NMO+DMO into three steps and to evaluate their contributions separately. Let the initial data be the zero-offset reflection event $\tau_0(x_0)$. The first step of the residual NMO+DMO is the inverse DMO operator. One can evaluate the effect of this operator by means of the offset continuation concept (Fomel, 2003a). According to this concept, each point of the input traveltime curve $\tau_0(x_0)$ travels with the change of the offset from zero to h along a special trajectory, which I call a *time ray*. Time rays are parabolic curves of the form

$$x(\tau) = x_0 + \frac{\tau^2 - \tau_0^2(x_0)}{\tau_0(x_0) \tau_0'(x_0)}, \quad (\text{B-1})$$

with the final points constrained by the equation

$$h^2 = \tau^2 \frac{\tau^2 - \tau_0^2(x_0)}{(\tau_0(x_0) \tau_0'(x_0))^2}, \quad (\text{B-2})$$

where $\tau_0'(x_0)$ is the derivative of $\tau_0(x_0)$. The second step of the cumulative residual NMO+DMO process is the residual normal moveout. According to equation (23), residual NMO is a one-trace operation transforming the traveltime τ to τ_1 as follows:

$$\tau_1^2 = \tau^2 + h^2 d, \quad (\text{B-3})$$

where

$$d = \left(\frac{1}{v_0^2} - \frac{1}{v_1^2} \right). \quad (\text{B-4})$$

The third step is dip moveout corresponding to the new velocity v_1 . DMO is the offset continuation from h to zero offset along the redefined time rays (Fomel, 2003a)

$$x_2(\tau_2) = x + \frac{hX}{\tau_1^2 H} (\tau_1^2 - \tau_2^2), \quad (\text{B-5})$$

where $H = \frac{\partial \tau_1}{\partial h}$, and $X = \frac{\partial \tau_1}{\partial x}$. The end points of the time rays (B-5) are defined by the equation

$$\tau_2^2 = -\tau_1^2 \frac{\tau_1 H}{h X^2}. \quad (\text{B-6})$$

The partial derivatives of the common-offset traveltimes are constrained by the offset continuation kinematic equation

$$h (H^2 - X^2) = \tau_1 H, \quad (\text{B-7})$$

which is equivalent to equation (A-12) in Appendix A. Additionally, as follows from equations (B-3) and the ray invariant equations from (Fomel, 2003a),

$$\tau_1 X = \tau \frac{\partial \tau}{\partial x} = \frac{\tau^2 \tau'_0(x_0)}{\tau_0(x_0)}. \quad (\text{B-8})$$

Substituting (B-1-B-4) and (B-7-B-8) into equations (B-5) and (B-6) and performing the algebraic simplifications yields the parametric expressions for velocity rays of the residual NMO+DMO process:

$$\begin{cases} x_2(d) = x_0 + \frac{h^2 \tau'_0(x_0)}{T} \left(1 - \frac{T^2}{T_2^2(d)}\right), \\ \tau(d) = \frac{\tau_1^2(d)}{T_2(d)}, \end{cases} \quad (\text{B-9})$$

where the function $T(h, \tau_0(x_0), \tau'_0(x_0))$ is defined by

$$T(h, \tau, \tau_x) = \frac{\tau + \sqrt{\tau^2 + 4h^2 \tau_x^2}}{2}, \quad (\text{B-10})$$

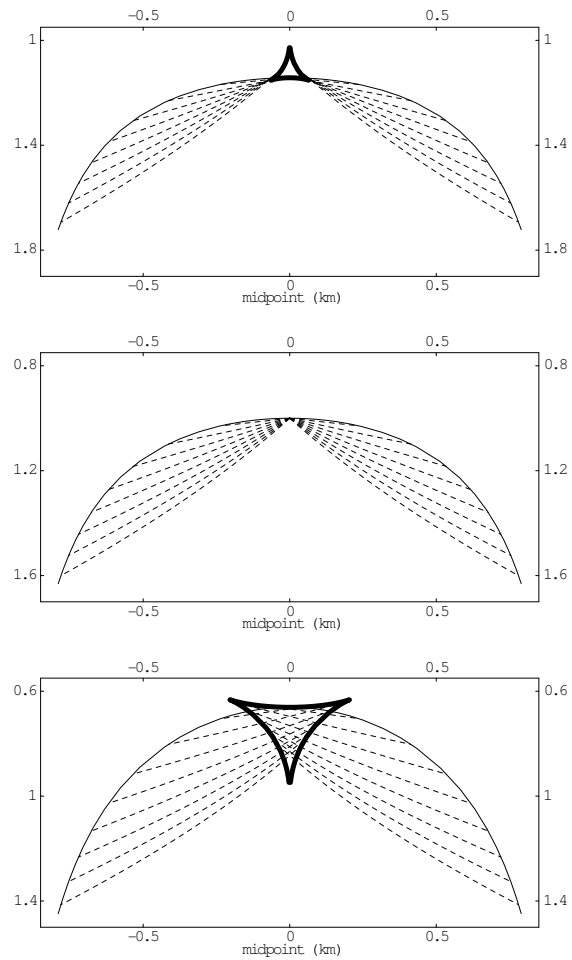
$$T_2(d) = \sqrt{T(h, \tau_1^2(d), \tau'_0(x_0)) T(h, \tau_0(x_0), \tau'_0(x_0))}, \quad (\text{B-11})$$

and

$$\tau_1^2(d) = \tau_0 T + d h^2. \quad (\text{B-12})$$

The last step of the cascade of inverse DMO, residual NMO, and DMO is illustrated in Figure B-1. The three plots in the figure show the offset continuation to zero offset of the inverse DMO impulse response shifted by the residual NMO operator. The middle plot corresponds to zero NMO shift, for which the DMO step collapses the wavefront back to a point. Both positive (top plot) and negative (bottom plot) NMO shifts result in the formation of the specific triangular impulse response of the residual NMO+DMO operator. As noticed by Etgen (1990), the size of the triangular operators dramatically decreases with the time increase. For large times (pseudo-depths) of the initial impulses, the operator collapses to a point corresponding to the pure NMO shift.

Figure B-1: Kinematic residual NMO+DMO operators constructed by the cascade of inverse DMO, residual NMO, and DMO. The impulse response of inverse DMO is shifted by the residual NMO procedure. Offset continuation back to zero offset forms the impulse response of the residual NMO+DMO operator. Solid lines denote traveltime curves; dashed lines denote the offset continuation trajectories (time rays). Top plot: $v_1/v_0 = 1.2$. Middle plot: $v_1/v_0 = 1$; the inverse DMO impulse response collapses back to the initial impulse. Bottom plot: $v_1/v_0 = 0.8$. The half-offset h in all three plots is 1 km.



APPENDIX C

INTEGRAL VELOCITY CONTINUATION AND KIRCHHOFF MIGRATION

The main goal of this appendix is to prove the equivalence between the result of zero-offset velocity continuation from zero velocity and conventional post-stack migration. After solving the velocity continuation problem in the frequency domain, I transform the solution back to the time-and-space domain and compare it with the conventional Kirchhoff migration operator (Schneider, 1978). The frequency-domain solution has its own value, because it forms the basis for an efficient spectral algorithm for velocity continuation (Fomel, 2003b).

Zero-offset migration based on velocity continuation is the solution of the boundary problem for equation (41) with the boundary condition

$$P|_{v=0} = P_0, \quad (\text{C-1})$$

where $P_0(t_0, x_0)$ is the zero-offset seismic section, and $P(t, x, v)$ is the continued wavefield. In order to find the solution of the boundary problem composed of (41) and (C-1), it is convenient to apply the function transformation $R(t, x, v) = tP(t, x, v)$, the time coordinate transformation $\sigma = t^2/2$, and, finally, the double Fourier transform over the squared time coordinate σ and the spatial coordinate x :

$$\widehat{R}(v) = \int \int P(t, x, v) \exp(i\Omega\sigma - ikx) t^2 dt dx. \quad (\text{C-2})$$

With the change of domain, equation (41) transforms to the ordinary differential equation

$$\frac{d\widehat{R}}{dv} = i \frac{k^2}{\Omega} v \widehat{R}, \quad (\text{C-3})$$

and the boundary condition (C-1) transforms to the initial value condition

$$\widehat{R}(0) = \widehat{R}_0, \quad (\text{C-4})$$

where

$$\widehat{R}_0 = \int \int P_0(t_0, x_0) \exp(i\Omega\sigma_0 - ikx_0) t_0^2 dt_0 dx_0, \quad (\text{C-5})$$

and $\sigma_0 = t_0^2/2$. The unique solution of the initial value (Cauchy) problem (C-3) - (C-4) is easily found to be

$$\widehat{R}(v) = \widehat{R}_0 \exp\left(i \frac{k^2}{2\Omega} v^2\right). \quad (\text{C-6})$$

In the transformed domain, velocity continuation appears to be a unitary phase-shift operator. An immediate consequence of this remarkable fact is the cascaded migration decomposition of post-stack migration (Larner and Beasley, 1987):

$$\exp\left(i \frac{k^2}{2\Omega} (v_1^2 + \cdots + v_n^2)\right) = \exp\left(i \frac{k^2}{2\Omega} v_1^2\right) \cdots \exp\left(i \frac{k^2}{2\Omega} v_n^2\right). \quad (\text{C-7})$$

Analogously, three-dimensional post-stack migration is decomposed into the two-pass procedure (Jakubowicz and Levin, 1983):

$$\exp\left(i \frac{k_1^2 + k_2^2}{2\Omega} v^2\right) = \exp\left(i \frac{k_1^2}{2\Omega} v^2\right) \exp\left(i \frac{k_2^2}{2\Omega} v^2\right). \quad (\text{C-8})$$

The inverse double Fourier transform of both sides of equality (C-6) yields the integral (convolution) operator

$$P(t, x, v) = \iint P_0(t_0, x_0) K(t_0, x_0; t, x, v) dt_0 dx_0, \quad (\text{C-9})$$

with the kernel K defined by

$$K = \frac{t_0^2/t}{(2\pi)^{m+1}} \iint \exp\left(i \frac{k^2}{2\Omega} v^2 + ik(x - x_0) - \frac{i\Omega}{2}(t^2 - t_0^2)\right) dk d\Omega, \quad (\text{C-10})$$

where m is the number of dimensions in x and k (m equals 1 or 2). The inner integral on the wavenumber axis k in formula (C-10) is a known table integral (Gradshteyn and Ryzhik, 1994). Evaluating this integral simplifies equation (C-10) to the form

$$K = \frac{t_0^2/t}{(2\pi)^{m/2+1} v^m} \int (i\Omega)^{m/2} \exp\left[\frac{i\Omega}{2}\left(t_0^2 - t^2 - \frac{(x - x_0)^2}{v^2}\right)\right] d\Omega. \quad (\text{C-11})$$

The term $(i\Omega)^{m/2}$ is the spectrum of the anti-causal derivative operator $\frac{d}{d\sigma}$ of the order $m/2$. Noting the equivalence

$$\left(\frac{\partial}{\partial\sigma}\right)^{m/2} = \left(\frac{1}{t} \frac{\partial}{\partial t}\right)^{m/2} = \left(\frac{1}{t}\right)^{m/2} \left(\frac{\partial}{\partial t}\right)^{m/2}, \quad (\text{C-12})$$

which is exact in the 3-D case ($m = 2$) and asymptotically correct in the 2-D case ($m = 1$), and applying the convolution theorem transforms operator (C-9) to the form

$$P(t, x, v) = \frac{1}{(2\pi)^{m/2}} \int \frac{\cos\alpha}{(v\rho)^{m/2}} \left(-\frac{\partial}{\partial t_0}\right)^{m/2} P_0\left(\frac{\rho}{v}, x_0\right) dx_0, \quad (\text{C-13})$$

where $\rho = \sqrt{v^2 t^2 + (x - x_0)^2}$, and $\cos\alpha = t_0/t$. Operator (C-13) coincides with the Kirchhoff operator of conventional post-stack time migration (Schneider, 1978).